PHILOSOPHICAL TRANSACTIONS OF THE ROYAL SOCIETY A MATHEMATICAL, PHYSICAL & ENGINEERING SCIENCES

Nano-/microstructure improved photocatalytic activities of semiconductors

Tianyi Zhao, Yong Zhao and Lei Jiang

Phil. Trans. R. Soc. A 2013 **371**, 20120303, published 2 September 2013

PHILOSOPHICAL TRANSACTIONS OF THE ROYAL SOCIETY A

rsta.royalsocietypublishing.org

Review

Cite this article: Zhao T, Zhao Y, Jiang L. 2013 Nano-/microstructure improved photocatalytic activities of semiconductors. Phil Trans R Soc A 371: 20120303. http://dx.doi.org/10.1098/rsta.2012.0303

One contribution of 17 to a Theme Issue 'Molecular nanostructure and nanotechnology'.

Subject Areas:
nanotechnology, photochemistry

Keywords:
photocatalysis, semiconductor, nano-/microstructure, structure-related properties

Author for correspondence:
Lei Jiang
e-mail: jianglei@buaa.edu.cn, jianglei@iccas.ac.cn

Nano-/microstructure improved photocatalytic activities of semiconductors

Tianyi Zhao[1], Yong Zhao[1] and Lei Jiang[1,2]

[1]Key Laboratory of Bio-Inspired Smart Interfacial Science and Technology of Ministry of Education, School of Chemistry and Environment, Beihang University, Beijing 100191, People's Republic of China
[2]Beijing National Laboratory for Molecular Sciences (BNLMS), Key Laboratory of Organic Solids, Institute of Chemistry, Chinese Academy of Sciences, Beijing 100190, People's Republic of China

Photocatalysis has emerged as a promising technique owing to its valuable applications in environmental purification. With the demand of building effective photocatalyst materials, semiconductor investigation experienced a developing process from simple chemical modification to complicated morphology design. In this review, the general relationship between morphology structures and photocatalytic properties is mainly discussed. Various nano-/microsized structures from zero- to three-dimensional are discussed, and the photocatalytic efficiency correspon- ding to the structures is analysed. The results showed that simple structures can be easily obtained and can facilitate chemical modification, whereas one- or three-dimensional structures can provide structure-enhanced properties such as surface area increase, multiple reflections of UV light, etc. Those principles of structure-related photocatalytic properties will afford basic ideology in designing new photocatalytic materials with more effective catalytic properties.

1. Introduction

Since the pioneering research of the photocatalytic splitting of water on TiO_2 electrodes by Fujishima & Honda [1], semiconductor materials with photocatalytic properties have attracted much interest as the requirements relating to increased organic pollutants become more stringent [2–7]. So far, a number of investigations

Royal Society Publishing
Informing the science of the future

have focused on the photocatalytic activities of various semiconductors, including ZnO, TiO_2, WO_3, Si, Fe_2O_3, CdS, ZnS, $SrTiO_3$, SnO_2, WSe_2 and so on, due to their good characteristics of strong oxidizing power, able to use visible and/or near-UV light, inexpensive and non-toxic [8–10]. However, photocatalytic activities of semiconductors are limited by several aspects, such as light absorption range, recycling of materials and production cost, and the major limitation is the high recombination rate of photoinduced electron–hole pairs that causes the relatively low value of quantum efficiency [11–17]. Therefore, enhancing the photocatalytic activity of semiconductors especially for visible-light irradiation becomes an imperative task for both the conversion of solar energy and the purification of the environment [11,18,19]. Some successful methods have been achieved and can be generally classified into two strategies which are using an organic dye as photosensitizer and doping with ions or other oxides. Both these two methods can directly modify the chemical composition of semiconductors; therefore, the photocatalytic response can be altered by chemical contents. Besides chemical methods, tuning physical morphology has also emerged as an efficient method to provide strongly enhanced photocatalytic properties by adjusting the size or structure of semiconductors.

In recent years (within the past 20–30 years), micro-/nanomaterials have drawn great attention worldwide and many efforts have been applied in a vast number of fields ranging from magnetic, electrical, optical, especially to photocatalytic activity [20–24]. Merging the micro-/ nanoscience and photocatalysis fields attracted continued interest because of their contributions to light energy harvesting compared with the bulk counterpart, and are expected to provide the basis for developing new and effective devices [25–27]. Various revolutionary research studies in both scientific and engineering fields have been reported focusing on the mechanisms and methodologies of the augment of photocatalytic activities [28–32]. In this review, we discuss the relationship between structure-induced photocatalytic properties of semiconductors, through summarizing the species of the structure types of semiconductors to highlight the special photocatalytic properties that are provided by nano-/microstructure, such as size quantization effects, structure-dependent crystallization, structure-induced multi-reflection effects and so on. The structure types of semiconductor materials can be sorted as zero-/two-dimensional, one-dimensional and multi-dimensional materials, according to their structural characteristics with the order from simple to complicated. The original generation (zero-dimensional) are solid membranes, films or powders, which initially gained researchers' attention because of their facile fabrications and easier utilization. Meanwhile, by further advancing such planar morphology involving porous or particle structures at the nanoscale, the band gap and the position of conducting and valence bands are strongly influenced, which is generally described as 'quantum size effect' [33–37]. The second generation can be considered as the semiconductor materials with one-dimensional well-organized geometrical shapes, such as nanorods, nanoparticles, nanowires (NWs), etc. Also hollow, porous or particle structures can be involved, which not only largely augment the surface area of the materials but also exhibit special characteristics such as higher efficiency of electron transport or easier substrate diffusion [38–41]. The third generation are semiconductors with hierarchical assemblies that combine the two- or three-dimensional structures. Such complicated structures further increase the surface area of semiconductor materials, and also show structure-induced characteristics such as multiple reflection of incident light, etc.

In this review, we will describe the synthetic techniques, the structure morphology and the structure-induced physical properties of semiconductors with photocatalytic activities. For better explanation, we categorize the semiconductors into three sorts by their structure type, and the benefits of each structure type are also illuminated. Table 1 presents the outline of this review.

2. Zero-/two-dimensional semiconductor materials

Basically, films and membranes are the most common and useful structures providing a two-dimensional planar morphology that can be easily covered on various substrates, and thereby

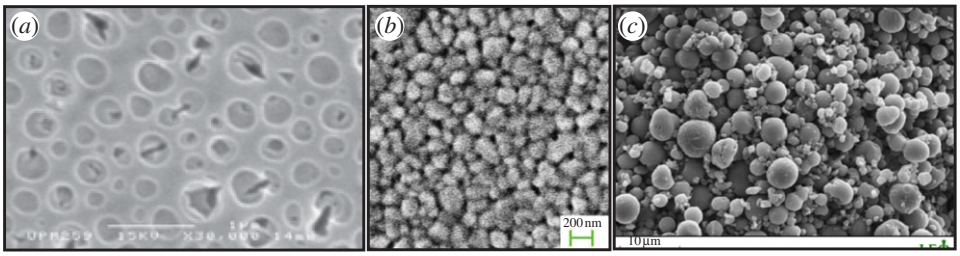

Figure 1. (*a*) TiO_2 thin films with microscaled pore structure; (*b*) scanning electron microscopy (SEM) image of the TiO_2 films composed of small nanoparticles; (*c*) typical SEM microphotograph of undoped TiO_2 particle. (Online version in colour.)

Table 1. The structure classification of photocatalytic semiconductors and their structure-enhanced photocatalytic types.

dimensional classification	significant structures	structure-induced contributions of photocatalysis
zero-/two-dimensional with simple structure	powder, film, membrane	quantum confinement effect, easier for doping and application
one-dimensional	nanotube, nanofibre, nanorod, etc.	augment of surface area, quantum confinement effect
multi-dimensional	micro-/nanocomposite structures	material composition, augment of surface area, multiple reflections of UV light, inner trap of pollutant

have been widely investigated by many researchers as the fundamental model. There are several techniques to form films coated on substrates, and can be generally categorized as dry processes (including reactive pulsed laser deposition [42], magnetron sputtering deposition and physical [43] or chemical vapour deposition [44,45]) and wet processes (including sol–gel technique [46–51], hydrothermal method [52] and micro-arc oxidation [53]). Among those preparation techniques, the sol–gel technique attracted lots of attention because of its simple operating process, low cost and it being able to effect large area coating [54,55]. The initial investigation of TiO_2 thin-film photocatalyst took place in the early 1990s, when Fujishima's group prepared a semitransparent TiO_2 film on a glass substrate by sintering a TiO_2 sol at 450°C. The prepared film showed extraordinarily high photocatalytic activity, even higher than that of one of the most active commercial TiO_2 powders, Degussa P-25 [56]. Owing to the development of special synthetic techniques, some micro-/nanostructures are being introduced into the film or membrane structures of semiconductors. For example, as shown in figure 1*a*, Zainal and Lee investigated the photoelectrocatalytic behaviour of sol–gel-derived TiO_2 thin films. The microscaled pore structures were obtained during the losing process of polyethylene glycol by heating treatment, and such sol–gel dip-coating method is effective to form well-covered and homogeneous films on the substrates [55].

Yu and Hu also prepared TiO_2 thin films on fused-SiO_2 substrates, by the sol–gel method and spin-coating technique. After calcinations, the continuous thin film was observed to consist of uniformly distributed small nanoparticles (as shown in figure 1*b*). Although the TiO_2 thin films were calcined at different temperature, the thickness of all the films was around 80 nm, and therefore showed transparent characteristics. The photocatalytic results also showed that the TiO_2 films prepared at 600 and 800°C possess the highest photocatalytic ability, owing to coarsening, crystal growth and spheroidizing of the TiO_2 grains in the films [54].

As the composition of the precursors for synthesizing films or membranes is easily controlled, transition metals [57,58] or other inorganic elements can simply be doped into films or membranes

to further adjust the photocatalytic activities of semiconductors. For example, Sayikan and co-workers synthesized Sn-doped and undoped nano-TiO_2 particles by hydrothermal process at low temperature, and transparent and smooth TiO_2-based thin films were further prepared by spin-coating technique. The photocatalytic performance of Sn-doped TiO_2 thin film is higher than that of undoped TiO_2 film (figure 1*c*) [59]. Kamat and co-workers have used nanostructured semiconductor films of SnO_2, TiO_2 and SnO_2/TiO_2 for the electrochemically assisted photocatalytic degradation of the textile azo dye naphthol blue black [60]. Recently, Yu's group synthesized a new family of lamellar transition-metal (Ni, Co) molybdate–cetyltrimethylammonium mesostructured composites by a simple chemical precipitation method, and these lamellar mesostructured composites displayed enhanced capability in decomposition of acid fuchsine [61]. Therefore, nanostructure as well as metal elements were involved in planar film forming porous or particle structures. Inorganic elements can also be doped into semiconductor materials for the potential better utilization of solar energy [62–65]. For example, Li *et al.* reported the synthesis of N-doped, F-doped and N–F-doped TiO_2 powders by spray pyrolysis and found that the N–F-doped TiO_2 demonstrated the highest visible-light activity [66]. Also due to the fact that films are easier to be synthesized and used, researchers usually choose such planar structures to examine the relationship between the crystal structure and photocatalytic property. For example, Yu and Hu investigated the relationship between the temperature-affected crystal structure and photocatalytic activities, finding that the anatase crystallites grow in size linearly with calcination temperature ranging from 600 to 1200°C, and the TiO_2 films prepared at 600–800°C possess higher photocatalytic ability than those prepared at 1000–1200°C [54]. Therefore, zero-dimensional planar bulk film or membrane provides a great contribution from fundamental researches of element-doping and crystal morphology of photocatalytic semiconductors to commercial products [67–69].

The above-mentioned nanostructured semiconductors can largely promote photocatalytic activity because of their unique properties derived from low dimensionality and quantum confinement effect. Indeed, the nano-sized materials with high surface areas exhibited enhanced photoactivities, because the photo-generated electron–hole pairs could move effectively to the surface to increase the number of active sites, and therefore the photocatalytic reaction would be enhanced markedly. On the other hand, the nanoscaled structure-induced quantum size effect will also promote the photocatalytic activity. For example, Hyeon and co-workers synthesized TiO_2 nanorods at a large scale via a non-hydrolytic ester elimination reaction of titanium(IV) alkoxide and oleic acid. After removing the stabilizing surfactants from the TiO_2 nanorods without aggregation, the naked nanorods were successfully prepared, and the photocatalytic inactivation was investigated. The results showed that the band gap shift of the TiO_2 nanorods should be attributed to the quantum size effect governed by the diameter of the nanorods (3.4 nm) rather than by their length (38 nm). The increased band gap of the TiO_2 nanorods partially enhanced photocatalytic activity [70]. Therefore, the introduction of nanosize into the conventional bulk semiconductors benefits their photocatalytic behaviour in a physical aspect. When downsizing the crystallite dimension of semiconductor particles up to several nanometres, the charge carriers appear to behave quantum mechanically [71–79], resulting in the increase of band gap and the shift of band edges to generate larger redox potential. Several studies have already found that using size-quantized semiconductors can enhance photoefficiencies [80–84], although other works showed that photoactivities of size-quantized semiconductors decreased compared with their bulk-phase counterparts [81,85]. Such phenomenon should be attributed to the competition relationship between the positive effects of increased potential on quantum yields and the unfavourable surface speciation and surface defects formed during the preparation processes of semiconductor particles [86–88].

3. One-dimensional semiconductor materials

Since the development of modern synthetic technologies and morphology observation equipment, various novel morphologies of nano-/microstructured semiconductors have been

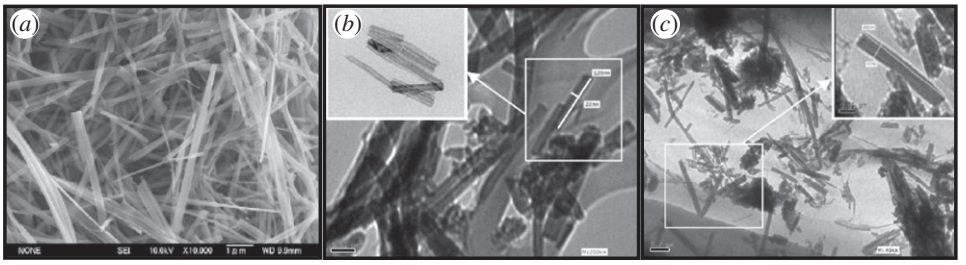

Figure 2. (*a*) SEM image of TiO_2 nanowires; (*b*) transmission electron microscopy (TEM) images of titanate nanotubes; (*c*) TEM images of TiO_2 nanorods.

prepared [89–92]. One-dimensional semiconductors, which possess nanoscaled section diameter and micro- or macroscaled length, have attracted considerable attention recently owing to their enhanced photocatalytic activities.

The basic category should be solid nanostructured semiconductor materials that are composed of the simplest units such as NWs and nanorods. For example, Yoshikawa's group synthesized TiO_2 NWs by the hydrothermal treatment of commercial TiO_2 powders (the scanning electron microscopy (SEM) structure is shown in figure 2*a*); meanwhile, the effect of post-heat-treatment temperature on the phase structure, morphology and photocatalytic activity for hydrogen evolution was investigated. Although the apparent one-dimensional morphology of TiO_2 NWs was thermally stable at any post-heat-treatment temperature, they presented different crystal structures from TiO_2(B) NWs (at approx. 300°C), to anatase-type (at approx. 500°C) to rutile-type (at more than 900°C). The order of the photocatalytic activity for H_2 evolution is: TiO_2 anatase > TiO_2 rutile ≥ TiO_2(B) > hydrogen titanate [93]. Recently, Yu's group prepared ultralong orthorhombic silver trimolybdate NWs with well-dispersed Ag nanoparticles by a simple hydrothermal process [94].

Hafez reported the large-scale synthesis of pure anatase TiO_2 nanorods (figure 2*c*) using a simple and low-cost modified hydrothermal method. The porous single-crystal TiO_2 nanorods have a good size distribution (approx. 4–16 nm) with the dimensions of 200–300 nm in length and of 30–50 nm in diameter, which resulted in high Brunauer–Emmett–Teller (BET) specific area of 85.2 $m^2\,g^{-1}$, and showed better environmental photocatalysis compared with their precursor nanostructures: (anatase/rutile) TiO_2 nanoparticles and titanate nanotubes (figure 2*b*) [95].

Various novel structures were introduced recently, because the nanostructures can largely enhance the photocatalytic activities of semiconductors. Wang's group reported a nanosheet morphology of titanium acid $H_2Ti_2O_5{\cdot}H_2O$ prepared by doping Zn^{2+} into Ti–O crystal structure through the hydrothermal method (figure 3*a*). Although the decomposition ratio of methyl orange solution with $H_2Ti_2O_5{\cdot}H_2O$ is slightly lower than that with TiO_2, the unique layer structure may still find much wider potential applications [96]. Xu and co-workers prepared uniformly sized anatase TiO_2 nanocrystallites with cuboidal morphology by changing titanium hydroxide precipitates into their corresponding ethanol gels, and then dried in supercritical ethanol and calcined at high temperature (figure 3*b*). This work also demonstrated that good crystallization of the material is crucial to photocatalytic ability, which was proved by the fact that increasing the calcination temperature up to 800°C improved the crystallization and further increased the photocatalytic activities [97]. Chen and co-workers synthesized pure brookite TiO_2 nanoflowers consisting of single crystalline nanorods by using a facile one-step hydrothermal process (figure 3*c*). The anatase, brookite and titanate can be adjusted by the concentration of NaCl during the hydrothermal treatment process, and the brookite nanoflowers exhibited remarkable photoactivity [98]. Caruso and co-workers demonstrated the novel use of a polymer gel template to produce TiO_2 networks with high porosity, which can be adjusted by the polymer gel properties from tens of nanometres to micrometres in diameter (figure 3*d*). Such open 'coral-like' network structure allows high access of the TiO_2 surface to the reaction medium, and shows high photocatalytic activity [99].

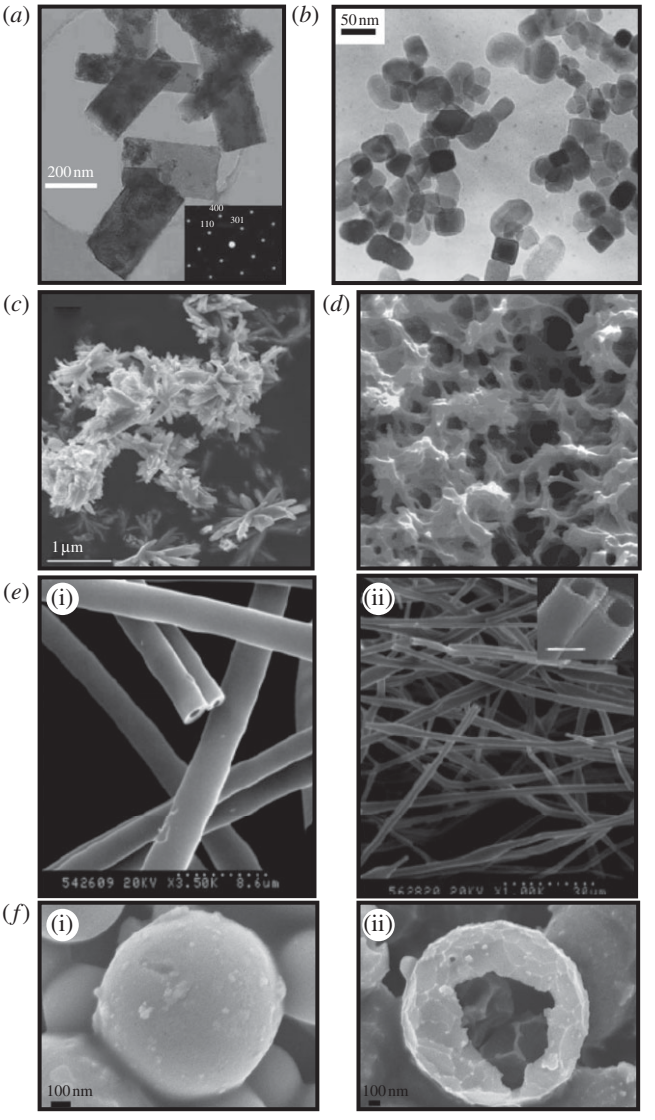

Figure 3. (*a*) Transmission electron microscopy (TEM) image and selected area electron diffraction pattern of as-prepared $H_2Ti_2O_5 \cdot H_2O$ with nanosheet structure. (*b*) TEM image of TiO_2 nanocuboids. (*c*) Field emission SEM image of brookite TiO_2 nanoflowers. (*d*) SEM image of TiO_2 networks with homogeneous pores. (*e*) SEM images of xerogel (i) and TiO_2 (ii) hollow fibres. (*f*) SEM images of hollow TiO_2 microsphere structures synthesized with the aerosol-assisted flow synthesis method: (i) B-doped and (ii) Ni-doped.

Furthermore, hollow structures were involved in one-dimensional morphology; therefore, nano-/microtubes, hollow spheres and core–shell structures were widely investigated. Chen's group prepared long TiO_2 hollow fibres with mesoporous walls by the sol–gel two-capillary spinneret electrospinning technique (figure 3*e*(i)(ii)). The porous fibres were as long as 30 cm with diameters of 0.1–4 µm and wall thicknesses of 60–500 nm, giving a BET surface area of 200–208 $m^2\,g^{-1}$ and an average pore size of 6.7 nm. These TiO_2 hollow fibres with mesoporous walls showed higher photocatalytic activities than commercial TiO_2 nanoparticles and corresponding mesoporous TiO_2 powders [100]. Crittenden's group also reported the preparation of a novel TiO_2-based p–n junction nanotube which combines the hollow structure and core–shell structure together. Platinum was contained in the hollow inner space of the

TiO_2-based nanotubes by a template and removing process. In this case, a p–n junction was built, and the electrons can move more freely in the platinum leaving more valence band holes in the TiO_2 [101].

Lee's group synthesized highly effective B-doped, Ni-doped and B–Ni-codoped TiO_2 microsphere photocatalysts via an aerosol-assisted flow synthesis method. The hollow structure (figure 3*f*(i)(ii)) was attributed to the escape of gas phase HBO_2 from the interior part of the TiO_2 microspheres during the pyrolysis reaction. The photocatalysis was enhanced, because the doping samples showed obvious red shift in their absorption edges [102].

Semiconductor materials of one-dimensional structure such as nanofibres and NWs, especially those with hollow structures such as nanotubes and hollow spheres, can also provide physical-enhanced photocatalytic activities besides enlarged photocatalytic surface area [38–41]. Tachikawa *et al.* have prepared titania nanotubes by digesting titania nanoparticles (e.g. P-25) under strong conditions in an autoclave [103]. Laser flash photolysis results showed that the half-life of the photo-generated holes was obviously longer for titania nanotubes compared with nanoparticle structures. Homoplastically, Yanagida *et al.* also claimed that the electron transport in titania nanotube electrodes was efficiently higher than in electrodes prepared with nanoparticles [104]. This should be attributed to the low dimensionality of the nanotube structures which resulted in the higher diffusion length of charge carriers. The results of parallel photocatalytic experiments in the presence or the absence of air revealed that the nanotube structures can generate more trapped electrons [103]. Schmuki and co-workers also claimed that the ordered tubes provide higher photocatalytic efficiency compared with P-25 films, and suggested that such a difference is due to an optimized photocatalyst geometry that favours substrate diffusion and diminishes the charge carriers [105]. Schmuki and co-workers reported that the potential of low dimensional hollow morphology in photocatalysis is very good, although more evidence is desirable. Therefore, improving the photocatalytic activities of semiconductors simply by changing the shape and dimension of materials has prodigious investigation values [106].

4. Multi-dimensional semiconductor materials

With the further development of synthetic techniques, hierarchical semiconductors with multi-dimensional morphology were fabricated with the expectation of better photocatalytic activities. The primary structure of these materials is based on nano- or microscaled aggregations, and then nanoparticle, nanoporous or other nanoscaled units comprise of the secondary structure. Therefore, the multi-dimensional semiconductor materials usually have micro-/nanocomposite structures, which will definitely further improve the surface area to promote the photocatalytic activities. Recently, many scientists focused their attention on the formation of multi-dimensional semiconductors and demonstrated that the catalytic process would occur more efficiently in hierarchical structures.

Through an electrospinning-assisted route, Wang and co-workers synthesized a three-dimensional Bi_2WO_6/TiO_2 hierarchical heterostructure. The Bi_2WO_6 nanoplates consist of nanoparticles with a size of less than 20 nm grown slantingly on the primary TiO_2 nanofibres. Compared with the bulk Bi_2WO_6/TiO_2 powder, the Bi_2WO_6 nanoparticles and the TiO_2 sample, the as-prepared hierarchical nanofibrous mat exhibited enhanced visible photocatalytic activity due to the structure–property relationships, including the surface area, grain size and hierarchical heterostructure (figure 4*a*) [107].

Yu and co-workers synthesized hierarchical nanoporous F-doped TiO_2 spheres by a one-step low-temperature hydrothermal approach. Therein, titanium tetrafluoride was used as both a source of fluorine doping and a precursor of titanium. During the hydrothermal process, HF was generated and created a localized HF-rich zone around the TiO_2 particles, which provided the nucleation centre and the chemical etching of the hydrolysis products; therefore, the hierarchical porous F-doped TiO_2 spheres were obtained. The as-prepared F-doped TiO_2 porous spheres

showed high photocatalytic activities, not only because the fluorine dopant shifted the optical absorption edge of TiO_2 to lower energies to enhance the photoactivities under visible light, but also it provided excellent adsorptive properties of chemical reactant, because the porous structure made it easy for molecules to move into or outside (figure 4*b*) [108].

Kale and co-workers prepared pretty marigold-like $CdIn_2S_4$ nanostructures and nanotubes using a hydrothermal method. The formation of the spherical (marigold flower) structure was mainly attributed to the geometric building blocks, because a simple array of such crystals (petals) will easily generate curvature and develop into a marigold-like structure. After the $CdIn_2S_4$ nanotube was formed in the methanol-mediated reaction, the curvature of the petals was further accelerated by the hydrothermal conditions. As the fascinating structure showed good crystallinity, H_2 production under visible-light irradiation was quite excellent and higher than those reported previously (figure 4*c*) [109].

Highly hierarchical plate-like $FeWO_4$ microcrystals have been synthesized by Yu and co-workers through a simple solvothermal route. The as-prepared product was composed of uniform hexangular plate-like microcrystals, each of which was composed of six nearly equal petals. Both the ethylene glycol and the concentration of CH_3COONa used in the preparation played an important role in the formation of plate-like $FeWO_4$ microcrystals, because the former can affect the solubility, reactivity and diffusion behaviour of the reagents, and the latter provides a basic environment for the formation of $FeWO_4$ microcrystals. The hierarchical $FeWO_4$ microstructures showed excellent photocatalytic activity in the degradation of organic contaminants under exposure to UV and visible-light irradiation (figure 4*d*) [110].

Zhang and co-workers reported hierarchical BiOX (X = Cl, Br, I) nanoplate microspheres that were synthesized by a general one-pot solvothermal process. The formation process of such hierarchical BiOX nanoplate microspheres was proposed to have three steps: first, the formation of BiOX nanoparticles; second, the ethylene glycol-induced self-assembly of primary nanoplates to form loose microspheres; third, the formation of regular hierarchical microspheres. Compared with TiO_2 (Degussa, P-25) under UV–visible light irradiation and C-doped TiO_2 under visible light, BiOI exhibited the most excellent activity under both UV–visible and visible-light irradiation because of its suitable band gap (figure 4*e*) [111].

Wu and co-workers synthesized facile and bioinspired ZnO hierarchical architectures, including prism-like and flower-like structures and crystalline and non-crystalline hollow microshperes, with the assistance of the amino acid histidine (His) under mild conditions. It is well known that histidine coordination to Zn^{2+} is a structural motif of zinc finger proteins [112–116], and histidine molecules play different roles in the formation and self-assembly of ZnO hierarchical architectures, owing to the competitive coordination between the histidine and OH^- to Zn^{2+} when the reactant molar ratios were adjusted. When Zn^{2+}/NaOH molar ratio is 1 : 22, OH^- plays the crucial role in controlling the growth, resulting in the formation of the anisotropic prism-like ZnO (figure 4*f*(i)). When Zn^{2+}/NaOH molar ratio is changed to 1 : 10 and 1 : 2.5, histidine molecules, as the competitive ligand of OH^- to Zn^{2+}, adsorb on the surface of ZnO nuclei and result in the formation of flower-like structures and nanoparticles (figure 4*f*(ii)), which further self-assembled into the hollow microspheres (figure 4*f*(iii)). When the Zn^{2+}/His molar ratio is changed to 1 : 2, ZnO nuclei are covered by the histidine molecules, which prevents further crystallization and results in the formation of the non-crystalline hollow microspheres (figure 4*f*(iv)). The as-prepared ZnO hierarchical architectures could photocatalyse the reaction of HCHO and CO_2 [117].

Xie's group synthesized a nanoplate-built hierarchical nest-like structure of Bi_2WO_6 by a facile and economical method in the presence of polyvinyl pyrrolidone, which acts as a selective crystal face inhibitor to align the nanoplates. During the formation of submicroscaled solid spheres by the aggregation of small primary nanocrystals, the free polymer molecules absorbed on the face of the submicroscaled solid spheres, which may provide many high-energy sites for further growth with prolonged hydrothermal treatment. Then, the hollow structures formed by growing of the submicroscaled solid spheres gradually inside the unstructured polymer aggregates.

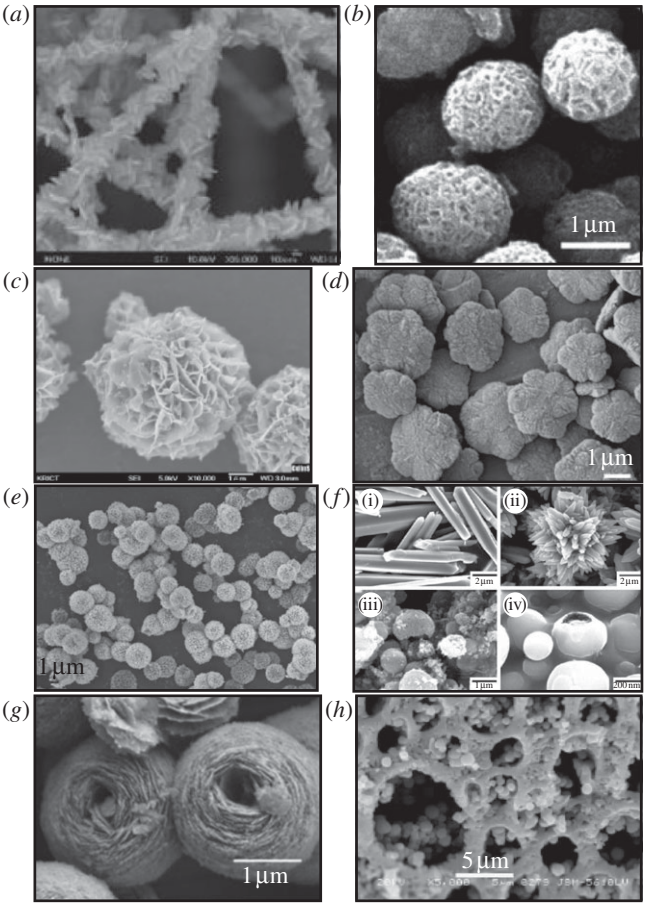

Figure 4. (*a*) The SEM image of a detailed view of Bi_2WO_6/TiO_2 hierarchical nanofibres. (*b*) SEM image of porous F-doped TiO_2 microspheres. (*c*) FE-SEM image of aqueous-mediated $CdIn_2S_4$ showing the marigold-like morphology. (*d*) FE-SEM image of hierarchical plate-like $FeWO_4$ microcrystals. (*e*) SEM image of BiOI microsphere powders. (*f*) Typical FE-SEM images of ZnO samples synthesized with Zn^{2+}/NaOH molar ratio of (i) 1 : 22, (ii) 1 : 10 and (iii) 1 : 2.5, the Zn^{2+}/His molar ratios were 1 : 1; (iv) 1 : 2.5 and Zn^{2+}/His molar ratio of 1 : 2. (*g*) Representative SEM image of Bi_2WO_6 hierarchical nest-like structures. (*h*) SEM image of as-prepared hierarchical macro-/mesoporous TiO_2 samples.

The hierarchical nest-like structure Bi_2WO_6 not only showed high photocatalytic activity but also exhibited a favourable discharge capacity in a lithium-ion battery [118].

Yu's group prepared a hierarchical macro/mesoporous titania using a micelle-templated method by the dropwise addition of tetrabutyl titanate to distilled water [119]. By hydrolyzation of tetrabutyl titanate in pure water, the water channels and the microphase-separated regions of TiO_2 particles were spontaneously radially patterned. The as-prepared hierarchical TiO_2 materials were calcined at different temperature, and the photocatalytic activities were evaluated. The results revealed that the hierarchical titania calcined at 300°C showed the most effective photocatalytic activity because of the best hierarchical macro-/mesoporous morphology and the largest specific surface area.

The major causation of the enhanced photoactivities of such complicated multi-dimensional semiconductors is still the augment of BET values compared with zero- or one-dimensional structures. However, besides surface area growth, such complicated structure of the multi-hierarchical materials also provides additional structure-induced properties such as extending the light absorption area into the visible region. For example, photonic crystals have been reported to promote light absorption by increasing the reflection of the light path when the incident light

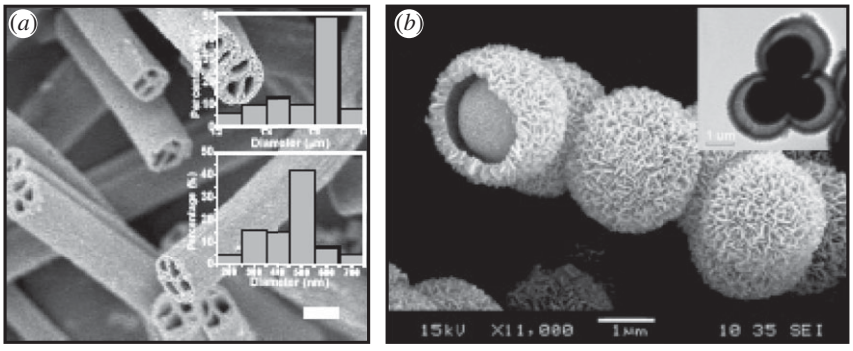

Figure 5. (*a*) SEM image of multichannel TiO_2 fibres; (*b*) SEM image of hollow titania spheres.

passes through the material [120–124]. The regularly ordered photonic crystals meant that it was difficult for the incident light to escape but was easily trapped inside the crystals when entering through them, and resulted in a multitude of reflections and diffractions. Therefore, the photonic crystal arrangement increased the probability of light absorption and charge separation by increasing the incident light contact time. On the other hand, inverse opals were reported to slow down photons and enhance the photocatalytic activities, because the dimension of the monodisperse empty spheres caused a light stop band at the wavelength relevant to the dimensions of the spheres [125]. Correspondingly, Jiang's group synthesized submicrosized multichannel TiO_2 fibres by multifluidic compound-jet electrospinning (figure 5*a*), which contain immiscible multichannel inner fluids and outer fluids. By removing the inner fluids through calcinations, the hollow multichannel structure was formed with controllable channel numbers by controlling the channel number of inner fluids. The photocatalytic activity evaluation revealed that the hollow structure can largely enhance the photoactivity because of the augmentation of surface area, and the hollow structure can also offer a cooperative effect of trapping more gaseous molecules inside the channels and multiple reflection of incident light [126]. Lu and Li reported the synthesis of hollow titania spheres with tunable interior structure and urchin-like morphology by a template-free approach (figure 5*b*), in which a titania precursor solvothermally reacted in glycerol, alcohol and ethyl ether. The photocatalytic activity results revealed that such unique structure can largely enhance the catalytic ability, because the sphere interior voids induced multiple reflections of UV light [127].

5. Conclusions

With the development of synthetic technology, several modification techniques and chemical additives have been developed to prepare semiconductors with various morphology from simple zero-dimensional to multi-dimensional. In addition, the research focuses experienced a transition from chemical doping to physical morphology designing to obtain better photocatalytic ability. In this review, the relationship between the photocatalytic properties of semiconductors and their physical microstructures was mainly discussed. An increasing amount of research has indicated that micro-/nanostructures can induce enhanced photocatalytic properties owing to their special configuration characteristics, revealing that one of the most important research areas in the future is the construction of micro-/nanocomposite materials. With the development of designing complicated structures of semiconductors, photocatalytic properties will be improved correspondingly; therefore, both experimental research and industrial applications will be benefited accordingly.

Funding statement. The authors thank the National Natural Science Foundation of China (grant nos. 21101010, 21222309, 21134003, 21004002), 973 Programme (nos. 2012CB933200, 2010CB934700, 2009CB30404) for continuing financial support.

References

1. Fujishima A, Honda K. 1972 Electrochemical photolysis of water at a semiconductor electrode. *Nature* **238**, 37–38. (doi:10.1038/238037a0)
2. Chen D, Ray AK, Appl B. 1999 Photocatalytic kinetics of phenol and its derivatives over UV irradiated TiO_2. *Appl. Catal. B* **23**, 143–157. (doi:10.1016/S0926-3373(99)00068-5)
3. Jing LQ, Xiaojun S, Jing S, Weimin C, Zili X, Yaoguo D, Honggang F. 2003 Review of surface photovoltage spectra of nano-sized semiconductor and its applications in heterogeneous photocatalysis. *Solar Energy Mater. Solar Cells* **79**, 133–151. (doi:10.1016/S0927-0248(02)00393-8)
4. Malato S, Blanco J, Vidal A, Richter C. 2002 Photocatalysis with solar energy at a pilot-plant scale: an overview. *Appl. Catal. B* **37**, 1–15. (doi:10.1016/S0926-3373(01)00315-0)
5. Rajeshwar K, de Tacconi NR, Chenthamarakshan CR. 2001 Semiconductor-based composite materials: preparation, properties, and performance. *Chem. Mater.* **13**, 2765–2782. (doi:10.1021/cm010254z)
6. Fujishima A, Rao TN, Tryk DA. 2000 Titanium dioxide photocatalysis. *J. Photochem. Photobiol. C* **1**, 1–21. (doi:10.1016/S1389-5567(00)00002-2)
7. Bi Y, Ouyang S, Umezawa N, Cao J, Ye J. 2011 Facet effect of single-crystalline Ag_3PO_4 sub-microcrystals on photocatalytic properties. *J. Am. Chem. Soc.* **133**, 6490–6492. (doi:10.1021/ja2002132)
8. Bhatkhande DS, Pangarkar VG, Beenackers A. 2002 Photocatalytic degradation for environmental applications: a review. *J. Chem. Technol. Biotechnol.* **77**, 102–116. (doi:10.1002/jctb.532)
9. Rajeshwar K. 1995 Photoelectrochemistry and the environment. *J. Appl. Electrochem.* **25**, 1067–1082. (doi:10.1007/BF00242533)
10. Hu B, Wu L-H, Liu S-J, Yao H-B, Shi H-Y, Li G-P, Yu S-H. 2010 Microwave-assisted synthesis of silver indium tungsten oxide mesocrystals and their selective photocatalytic properties. *Chem. Commun.* **46**, 2277–2279. (doi:10.1039/b921455k)
11. Kitano M, Matsuoka M, Ueshima M, Anpo M. 2007 Recent developments in titanium oxide-based photocatalysts. *Appl. Catal. A* **325**, 1–14. (doi:10.1016/j.apcata.2007.03.013)
12. Thu HB, Karkmaz M, Puzenat E, Guillard C, Herrmann J-M. 2005 From the fundamentals of photocatalysis to its applications in environment protection and in solar purification of water in arid countries. *Res. Chem. Intermediates* **31**, 449–461. (doi:10.1163/1568567053956671)
13. Schiavello M. 1988 Photocatalysis and environment: trends and applications. *NATO ASI Ser. C, Math. Phys. Sci.* **237**, 351.
14. Legrini O, Oliveros E, Braun AM. 1993 Photochemical processes for water treatment. *Chem. Rev.* **93**, 671–698. (doi:10.1021/cr00018a003)
15. Fox MA, Dulay MT. 1993 Heterogeneous photocatalysis. *Chem. Rev.* **93**, 341–357. (doi:10.1021/cr00017a016)
16. Pichat P, Guillard C, Maillard C, Amalric L, D'Oliveira JC. 1993 TiO_2 photocatalytic destruction of water aromatic pollutants. In *Photocatalytic purification and treatment of water and air* (eds DF Ollis, H Al-Ekabi), pp. 207–223. Amsterdam, The Netherlands: Elsevier.
17. Cunningham J, Sayyed GA, Sedlak P, Caffrey J. 1999 Aerobic and anaerobic TiO_2-photocatalysed purification of water containing organic pollutants. *Catal. Today* **53**, 145–158. (doi:10.1016/S0920-5861(99)00109-1)
18. Yamashita H, Takeuchi M, Anpo M. 2004 Visible-light-sensitive photocatalysts. *Encylopedia Nanosci. Nanotechnol.* **10**, 639–654.
19. Kisch H, Macyk W. 2002 Visible-light photocatalysis by modified titania. *Chem. Phys. Chem.* **3**, 399–400. (doi:10.1002/1439-7641(20020517)3:5<399::AID-CPHC399>3.0.CO;2-H)
20. Gao M-R, Xu Y-F, Jiang J, Shu-Hong Yu 2013 Nanostructured metal chalcogenides: synthesis, modification, and applications in energy conversion and storage devices. *Chem. Soc. Rev.* **42**, 2986–3017. (doi:10.1039/c2cs35310e)
21. Aldakov D, Lefrancois A, Reiss P. 2013 Ternary and quaternary metal chalcogenide nanocrystals: synthesis, properties and applications. *J. Mater. Chem. C* **1**, 3756–3776. (doi:10.1039/c3tc30273c)
22. Lai X, Halpert JE, Wang D. 2012 Recent advances in micro-/nano-structured hollow spheres for energy applications: from simple to complex systems. *Energy Environ. Sci.* **5**, 5604–5618. (doi:10.1039/c1ee02426d)

23. Zhao Y, Jiang L. 2009 Hollow micro/nanomaterials with multilevel interior structures. *Adv. Mater.* **21**, 3621–3638. (doi:10.1002/adma.200803645)
24. Zhang L, Zhou Q, Liu Z, Hou X, Li Y, Lv Y. 2009 Novel Mn_3O_4 micro-octahedra: promising cataluminescence sensing material for acetone. *Chem. Mater.* **21**, 5066–5071. (doi:10.1021/cm901369u)
25. Nagai H, Irie T, Takahashi J, Wakida S-I. 2007 Flexible manipulation of microfluids using optically regulated adsorption/desorption of hydrophobic materials. *Biosens. Bioelectron.* **22**, 1968–1973. (doi:10.1016/j.bios.2006.08.037)
26. Xu JJ, Ao Y, Fu D, Yuan C. 2008 Synthesis of Bi_2O_3–TiO_2 composite film with high-photocatalytic activity under sunlight irradiation. *Appl. Surf. Sci.* **255**, 2365–2369. (doi:10.1016/j.apsusc.2008.07.095)
27. Bai H, Liu Z, Sun DD. 2010 Hierarchically multifunctional TiO_2 nano-thorn membrane for water purification. *Chem. Commun.* **46**, 6542–6544. (doi:10.1039/c0cc01143f)
28. Maness PC *et al.* 1999 Bactericidal activity of photocatalytic TiO_2 reaction: toward an understanding of its killing mechanism. *Appl. Environ. Microbiol.* **65**, 4094–4098.
29. Stylidi M, Kondarides DI, Verykios XE. 2003 Pathways of solar light-induced photocatalytic degradation of azo dyes in aqueous TiO_2 suspensions. *Appl. Catal. B* **40**, 271–286. (doi:10.1016/S0926-3373(02)00163-7)
30. Sunada K, Watanabe T, Hashimoto K. 2003 Studies on photokilling of bacteria on TiO_2 thin film. *J. Photochem. Photobiol. A* **156**, 227–233. (doi:10.1016/S1010-6030(02)00434-3)
31. Diwald O, Thompson TL, Goralski EG, Walck SD, Yates JT. 2004 The effect of nitrogen ion implantation on the photoactivity of TiO_2 rutile single crystals. *J. Phys. Chem. B* **108**, 52–57. (doi:10.1021/jp030529t)
32. Bavykin DV, Friedrich JM, Walsh FC. 2006 Protonated titanates and TiO_2 nanostructured materials: synthesis, properties, and applications. *Adv. Mater.* **18**, 2807–2824. (doi:10.1002/adma.200502696)
33. Anpo M, Yamashita H, Ichihashi Y, Fujii Y, Honda M. 1997 Photocatalytic reduction of CO_2 with H_2O on titanium oxides anchored with micropores of zeolites: effects of the structure of the active sites and the addition of Pt. *J. Phys. Chem. B* **101**, 2632–2636. (doi:10.1021/jp962696h)
34. Lassaletta G, Fernandez A, Espinos JP, Gonzalez-Elipe AR. 1995 Spectroscopic characterization of quantum-sized TiO_2 supported on silica: influence of size and TiO_2–SiO_2 interface composition. *J. Phys. Chem.* **99**, 1484–1490. (doi:10.1021/j100005a019)
35. Kormann C, Bahnemann DW, Hoffmann MR. 1988 Preparation and characterization of quantum-size titanium dioxide. *J. Phys. Chem.* **92**, 5196–5201. (doi:10.1021/j100329a027)
36. Tolbert SH, Herhold A, Johnson C, Alivisatos A. 1994 Comparison of quantum confinement effects on the electronic absorption spectra of direct and indirect gap semiconductor nanocrystals. *Phys. Rev. Lett.* **73**, 3266–3269. (doi:10.1103/PhysRevLett.73.3266)
37. Henglein A. 1989 Small-particle research: physicochemical properties of extremely small colloidal metal and semiconductor particles. *Chem. Rev.* **89**, 1861–1873. (doi:10.1021/cr00098a010)
38. McCann JT, Marquez M, Xia Y. 2006 Melt coaxial electrospinning: a versatile method for the encapsulation of solid materials and fabrication of phase change nanofibers. *Nano Lett.* **6**, 2868–2872. (doi:10.1021/nl0620839)
39. Song ZQ, Xu HY, Li KW, Wang H, Yan H. 2005 Hydrothermal synthesis and photocatalytic properties of titanium acid $H_2Ti_2O_5 \cdot H_2O$ nanosheets. *J. Mol. Catal. A* **239**, 87–91. (doi:10.1016/j.molcata.2005.06.005)
40. Xiong C, Balkus JKJ. 2005 Fabrication of TiO_2 nanofibers from a mesoporous silica film. *Chem. Mater.* **17**, 5136–5140. (doi:10.1021/cm050819h)
41. Yuan Z-Y, Su B-L. 2004 Titanium oxide nanotubes, nanofibers and nanowires. *Colloids Surf. A* **241**, 173–183. (doi:10.1016/j.colsurfa.2004.04.030)
42. Xu Y, Shen M. 2008 Fabrication of anatase-type TiO_2 films by reactive pulsed laser deposition for photocatalyst application. *J. Mater. Process. Technol.* **202**, 301–306. (doi:10.1016/j.jmatprotec.2007.09.015)
43. Wenbin X, Shurong D, Demiao W, Gaochao R. 2008 Investigation of microstructure evolution in Pt-doped TiO_2 thin films deposited by RF magnetron sputtering. *Physica B* **403**, 2698–2701. (doi:10.1016/j.physb.2008.01.048)

44. Gröler T, Zeiler E, Franz A, Plewa O, Rosiwal SM, Singer RF. 1999 Erosion resistance of CVD diamond-coated titanium alloy for aerospace applications. *Surf. Coat. Technol.* **112**, 129–132. (doi:10.1016/S0257-8972(98)00800-7)
45. Gruss KA, Davis RF. 1999 Adhesion measurement of zirconium nitride and amorphous silicon carbide coatings to nickel and titanium alloys. *Surf. Coat. Technol.* **114**, 156–168. (doi:10.1016/S0257-8972(99)00042-0)
46. Yoko T, Hu L, Kozuka H, Sakka S. 1996 Photoelectrochemical properties of TiO_2 coating films prepared using different solvents by the sol–gel method. *Thin Solid Films* **283**, 188–195. (doi:10.1016/0040-6090(95)08222-0)
47. Yu J, Zhao X, Zhao Q. 2000 Effect of surface structure on photocatalytic activity of TiO_2 thin films prepared by sol–gel method. *Thin Solid Films* **379**, 7–14. (doi:10.1016/S0040-6090(00)01542-X)
48. Lu C-H, Wu W-H, Kale RB. 2007 Synthesis of photocatalytic TiO_2 thin films via the high-pressure crystallization process at low temperatures. *J. Hazardous Mater.* **147**, 213–218. (doi:10.1016/j.jhazmat.2006.12.068)
49. Zhang W *et al.* 2008 Preparation and antibacterial behavior of Fe^{3+}-doped nanostructured TiO_2 thin films. *Thin Solid Films* **516**, 4690–4694. (doi:10.1016/j.tsf.2007.08.053)
50. Chang C-C, Chen Y, Yu S, Chen S, Yin Y. 2008 Photocatalytic properties of porous TiO_2/Ag thin films. *Thin Solid Films* **516**, 1743–1747. (doi:10.1016/j.tsf.2007.05.033)
51. Epifani M, Helwig A, Arbiol J, Daz J, Francioso L, Siciliano P, Mueller G, Morante JR. 2008 TiO_2 thin films from titanium butoxide: synthesis, Pt addition, structural stability, microelectronic processing and gas-sensing properties. *Sens. Actuators B* **130**, 599–608. (doi:10.1016/j.snb.2007.10.016)
52. Miyauchi M, Tokudome H. 2007 Super-hydrophilic and transparent thin films of TiO_2 nanotube arrays by a hydrothermal reaction. *J. Mater. Chem.* **17**, 2095–2100. (doi:10.1039/b700387k)
53. Jin F, Chu PK, Wang K, Zhao J, Huang A, Tong H. 2008 Thermal stability of titania films prepared on titanium by micro-arc oxidation. *Mater. Sci. Eng. A* **476**, 78–82. (doi:10.1016/j.msea.2007.05.070)
54. Yu H-F, Hu F-C. 2009 Preparation and characterization of transparent TiO_2 thin films coated on fused-silica substrates. *J. Sol–Gel Sci. Technol.* **52**, 158–165. (doi:10.1007/s10971-009-2005-3)
55. Zainal Z, Lee CY. 2006 Properties and photoelectrocatalytic behaviour of sol–gel derived TiO_2 thin films. *J. Sol–Gel Sci. Technol.* **37**, 19–25. (doi:10.1007/s10971-005-4890-4)
56. Sopyan I, Watanabe M, Murasawa S, Hashimoto K, Fujishima A. 1996 An efficient TiO_2 thin-film photocatalyst: photocatalytic properties in gas-phase acetaldehyde degradation. *J. Photochem. Photobiol. A* **98**, 79–86. (doi:10.1016/1010-6030(96)04328-6)
57. Ghosh AK, Maruska HP. 1977 Photoelectrolysis of water in sunlight with sensitized semiconductor electrodes. *J. Electrochem. Soc.* **124**, 1516–1522. (doi:10.1149/1.2133104)
58. Anpo M. 1997 Photocatalysis on titanium oxide catalysts: approaches in achieving highly efficient reactions and realizing the use of visible light. *Catal. Surv. Jpn* **1**, 169–179. (doi:10.1023/A:1019024913274)
59. Arpac E, Sayilkan F, Asilturk M, Tatar P, Kiraz N, Sayilkan H. 2007 Photocatalytic performance of Sn-doped and undoped TiO_2 nanostructured thin films under UV and vis-lights. *J. Hazardous Mater.* **140**, 69–74. (doi:10.1016/j.jhazmat.2006.06.057)
60. Jing L, Xiaojun S, Weimin C, Zili X, Yaoguo D, Honggang F. 2003 The preparation and characterization of nanoparticle TiO_2/Ti films and their photocatalytic activity. *J. Phys. Chem. Solids* **64**, 615–623. (doi:10.1016/S0022-3697(02)00362-1)
61. Yao H-B, Li X-B, Liu S-J, Yu S-H. 2009 Lamellar transition-metal molybdate-CTA mesostructured composites (metal = Ni, Co): one-pot synthesis and application in treatment of acid fuchsine. *Chem. Commun.* 6732–6734. (doi:10.1039/b914329g)
62. Asahi R *et al.* 2001 Visible-light photocatalysis in nitrogen-doped titanium oxides. *Science* **293**, 269–271. (doi:10.1126/science.1061051)
63. Yao KS, Wang Y, Ho WY, Yan JJ, Tzeng KC. 2007 Photocatalytic bactericidal effect of TiO_2 thin film on plant pathogens. *Surf. Coat. Technol.* **201**, 6886–6888. (doi:10.1016/j.surfcoat.2006.09.068)
64. Khan SUM, Al-Shahry M, Ingler WB. 2002 Efficient photochemical water splitting by a chemically modified *n*-TiO_2. *Science* **297**, 2243–2245. (doi:10.1126/science.1075035)

65. Ohno T, Akiyoshi M, Umebayashi T, Asai K, Mitsui T, Matsumura M. 2004 Preparation of S-doped TiO_2 photocatalysts and their photocatalytic activities under visible light. *Appl. Catal. A* **265**, 115–121. (doi:10.1016/j.apcata.2004.01.007)
66. Li D, Ohashi N, Hishita S, Kolodiazhnyi T, Haneda H. 2005 Origin of visible-light-driven photocatalysis: a comparative study on N/F-doped and N–F-codoped TiO_2 powders by means of experimental characterizations and theoretical calculations. *J. Solid State Chem.* **178**, 3293–3302. (doi:10.1016/j.jssc.2005.08.008)
67. Fujishima A, Hashimoto K, Watanabe T. 1999 *TiO_2 photocatalysis: fundamentals and applications*. Tokyo, Japan: BKC.
68. Heller A. 1995 Chemistry and applications of photocatalytic oxidation of thin organic films. *Acc. Chem. Res.* **28**, 503–508. (doi:10.1021/ar00060a006)
69. Honda H, Ishizaki A, Soma R, Hashimoto K, Fujishima A. 1998 Application of photocatalytic reactions caused by TiO_2 film to improve the maintenance of factor of lighting system. *J. Illum. Eng. Soc.* **27**, 42–49.
70. Joo J *et al.* 2005 Large-scale synthesis of TiO_2 nanorods via nonhydrolytic sol–gel ester elimination reaction and their application to photocatalytic inactivation of *E. coli*. *J. Phys. Chem. B* **109**, 15 297–15 302. (doi:10.1021/jp052458z)
71. Kamat PV. 1993 Photochemistry on nonreactive and reactive (semiconductor) surfaces. *Chem. Rev.* **93**, 267–300. (doi:10.1021/cr00017a013)
72. Brus L. 1991 Quantum crystallites and nonlinear optics. *Appl. Phys. A* **53**, 465–474. (doi:10.1007/BF00331535)
73. Weller H. 1993 Quantized semiconductor particles: a novel state of matter for materials science. *Adv. Mater.* **5**, 88–95. (doi:10.1002/adma.19930050204)
74. Weller H. 1993 Colloidal semiconductor Q-particles: chemistry in the transition region between solid state and molecules. *Angew. Chem. Int. Ed.* **32**, 41–53. (doi:10.1002/anie.199300411)
75. Grätzel M. 1991 All surface and no bulk. *Nature* **349**, 740–741. (doi:10.1038/349740a0)
76. Henglein A. 1988 Mechanism of reactions on colloidal microelectrodes and size quantization effects. *Top. Curr. Chem.* **143**, 113–180. (doi:10.1007/BFb0018073)
77. Steigerwald ML, Brus LE. 1989 Synthesis, stabilization, and electronic structure of quantum semiconductor nanoclusters. *Annu. Rev. Mater. Sci.* **19**, 471–495. (doi:10.1146/annurev.ms.19.080189.002351)
78. Steigerwald ML *et al.* 1988 Surface derivatization and isolation of semiconductor cluster molecules. *J. Am. Chem. Soc.* **110**, 3046–3050. (doi:10.1021/ja00218a008)
79. Bawendi MG, Steigerwald ML, Brus LE. 1990 The quantum mechanics of larger semiconductor clusters ('quantum dots'). *Annu. Rev. Phys. Chem.* **41**, 477–496. (doi:10.1146/annurev.pc.41.100190.002401)
80. Hoffmann AJ, Carraway ER, Hoffmann MR. 1988 Photocatalytic production of H_2O_2 and organic peroxides in aqueous suspensions of TiO_2, ZnO, and desert sand. *Environ. Sci. Technol.* **22**, 798–806. (doi:10.1021/es00172a009)
81. Hoffman AJ, Mills G, Yee H, Hoffmann MR. 1992 Q-sized cadmium sulfide: synthesis, characterization, and efficiency of photoinitiation of polymerization of several vinylic monomers. *J. Phys. Chem.* **96**, 5546–5552. (doi:10.1021/j100192a067)
82. Anpo M, Shima T, Kodama S, Kubokawa Y. 1987 Photocatalytic hydrogenation of propyne with water on small-particle titania: size quantization effects and reaction intermediates. *J. Phys. Chem.* **91**, 4305–4310. (doi:10.1021/j100300a021)
83. Nedeljkovic JM, Nenadovic MT, Micic OI, Nozik AJ. 1986 Enhanced photoredox chemistry in quantized semiconductor colloids. *J. Phys. Chem.* **90**, 12–13. (doi:10.1021/j100273a005)
84. Nosaka Y, Ohta N, Miyama H. 1990 Photochemical kinetics of ultrasmall semiconductor particles in solution: effect of size on the quantum yield of electron transfer. *J. Phys. Chem.* **94**, 3752–3755. (doi:10.1021/j100372a073)
85. Giuseppe P, Langford CH, Vichova J, Vicek A. 1993 Photochemistry and picosecond absorption spectra of aqueous suspensions of a polycrystalline titanium oxide optically transparent in the visible spectrum. *J. Photochem. Photobiol. A* **75**, 67–75. (doi:10.1016/1010-6030(93)80161-2)
86. Faust BC, Hoffmann MR, Bahnemann DW. 1989 Photocatalytic oxidation of sulfur dioxide in aqueous suspensions of alpha iron oxide (Fe_2O_3). *J. Phys. Chem.* **93**, 6371–6381. (doi:10.1021/j100354a021)

87. Nishimoto S, Ohtani B, Kajiwara H, Kagiya T. 1985 Correlation of the crystal structure of titanium dioxide prepared from titanium tetra-2-propoxide with the photocatalytic activity for redox reactions in aqueous propan-2-ol and silver salt solutions. *J. Chem. Soc. Faraday Trans. 1* **81**, 61–68. (doi:10.1039/F19858100061)
88. Lee W *et al.* 1992 Preparation and characterization of titanium (IV) oxide photocatalysts. *Mater. Res. Bull.* **27**, 685–692. (doi:10.1016/0025-5408(92)90075-B)
89. Yoo S, Akbar SA, Sandhage KH. 2004 Nanocarving of bulk titania crystals into oriented arrays of single-crystal nanofibers via reaction with hydrogen-bearing gas. *Adv. Mater.* **16**, 260–264. (doi:10.1002/adma.200305781)
90. Imai H, Takei Y, Shimizu K, Matsuda M, Hirashima H. 1999 Direct preparation of anatase TiO_2 nanotubes in porous alumina membranes. *J. Mater. Chem.* **9**, 2971–2972. (doi:10.1039/A906005G)
91. Kasuga T, Hiramatsu M, Hoson A, Sekino T, Niihara K. 1999 Titania nanotubes prepared by chemical processing. *Adv. Mater.* **11**, 1307–1311. (doi:10.1002/(SICI)1521-4095(199910)11:15<1307::AID-ADMA1307>3.0.CO;2-H)
92. Zhou Y-X, Yao H-B, Yao W-T, Zhu Z, Yu S-H. 2012 Sacrificial templating synthesis of hematite nanochains from $[Fe_{18}S_{25}]$(TETAH)14 nanoribbons: their magnetic, electrochemical, and photocatalytic properties. *Chem. Eur. J.* **18**, 5073–5079. (doi:10.1002/chem.201102736)
93. Jitputti J, Suzuki Y, Yoshikawa S. 2008 Synthesis of TiO_2 nanowires and their photocatalytic activity for hydrogen evolution. *Catal. Commun.* **9**, 1265–1271. (doi:10.1016/j.catcom.2007.11.016)
94. Feng M, Song J-M, Li X-G, Yu S-H. 2011 Ultralong silver trimolybdate nanowires: synthesis, phase transformation, stability, and their photocatalytic, optical, and electrical properties. *ACS Nano* **5**, 6726–6735. (doi:10.1021/nn202296h)
95. Hafez HS. 2009 Synthesis of highly-active single-crystalline TiO_2 nanorods and its application in environmental photocatalysis. *Mater. Lett.* **63**, 1471–1474. (doi:10.1016/j.matlet.2009.03.057)
96. Song Z, Xu HY, Li KW, Wang H, Yan H. 2005 Hydrothermal synthesis and photocatalytic properties of titanium acid $H_2Ti_2O_5{\cdot}H_2O$ nanosheets. *J. Mol. Catal. A* **239**, 87–91. (doi:10.1016/j.molcata.2005.06.005)
97. Wang H, Wu Y, Xu B-Q. 2005 Preparation and characterization of nanosized anatase TiO_2 cuboids for photocatalysis. *Appl. Catal. B* **59**, 139–146. (doi:10.1016/j.apcatb.2005.02.001)
98. Zhao B *et al.* 2009 Brookite TiO_2 nanoflowers. *Chem. Commun.* 5115–5117. (doi:10.1039/b909883f)
99. Caruso RA, Antonietti M, Giersig M, Hentze H-P, Jia J. 2001 Modification of TiO_2 network structures using a polymer gel coating technique. *Chem. Mater.* **13**, 1114–1123. (doi:10.1021/cm001222z)
100. Zhan S, Chen D, Jiao X, Tao C. 2006 Long TiO_2 hollow fibers with mesoporous walls: sol-gel combined electrospun fabrication and photocatalytic properties. *J. Phys. Chem. B* **110**, 11 199–11 204. (doi:10.1021/jp057372k)
101. Chen YS, Crittenden JC, Hackney S, Sutter L, Hand DW. 2005 Preparation of a novel TiO_2-based p–n junction nanotube photocatalyst. *Environ. Sci. Technol.* **39**, 1201–1208. (doi:10.1021/es049252g)
102. Huang Y, Ho W, Ai Z, Song X, Zhang L, Lee S. 2009 Aerosol-assisted flow synthesis of B-doped, Ni-doped and B–Ni-codoped TiO_2 solid and hollow microspheres for photocatalytic removal of NO. *Appl. Catal. B* **89**, 398–405. (doi:10.1016/j.apcatb.2008.12.020)
103. Tachikawa T, Fujitsuka M, Majima T. 2007 Mechanistic insight into the TiO_2 photocatalytic reactions: design of new photocatalysts. *J. Phys. Chem. C* **111**, 5259–5275. (doi:10.1021/jp069005u)
104. Ohsaki Y, Masaki N, Kitamura T, Wada Y, Okamoto T, Sekino T, Niihara K, Yanagida S. 2005 Dye-sensitized TiO_2 nanotube solar cells: fabrication and electronic characterization. *Phys. Chem. Chem. Phys.* **7**, 4157–4163. (doi:10.1039/b511016e)
105. Macak JM, Zlamal M, Krysa J, Schmuki P. 2007 Self-organized TiO_2 nanotube layers as highly efficient photocatalysts. *Small* **3**, 300–304. (doi:10.1002/smll.200600426)
106. Aprile C, Corma A, Garcia H. 2008 Enhancement of the photocatalytic activity of TiO_2 through spatial structuring and particle size control: from subnanometric to submillimetric length scale. *Phys. Chem. Chem. Phys.* **10**, 769–783. (doi:10.1039/b712168g)

107. Shang M, Wang W, Zhang L, Sun S, Wang L, Zhou L. 2009 3D Bi_2WO_6/TiO_2 hierarchical heterostructure: controllable synthesis and enhanced visible photocatalytic degradation performances. *J. Phys. Chem. C* **113**, 14 727–14 731. (doi:10.1021/jp9045808)
108. Ho W, Yu JC, Lee S. 2006 Synthesis of hierarchical nanoporous F-doped TiO_2 spheres with visible light photocatalytic activity. *Chem. Commun.* 1115–1117. (doi:10.1039/B515513D)
109. Kale BB, Baeg J-O, Lee SM, Chang H, Moon S-J, Lee CW. 2006 $CdIn_2S_4$ nanotubes and 'marigold' nanostructures: a visible-like photocatalyst. *Adv. Funct. Mater.* **16**, 1349–1354. (doi:10.1002/adfm.200500525)
110. Zhou Y-X, Yao H-B, Zhang Q, Gong J-Y, Liu S-J, Yu S-H. 2009 Hierarchical $FeWO_4$ microcrystals: solvothermal synthesis and their photocatalytic and magnetic properties. *Inorg. Chem.* **48**, 1082–1090. (doi:10.1021/ic801806r)
111. Zhang X, Ai Z, Jia F, Zhang L. 2008 Generalized one-pot synthesis, characterization, and photocatalytic activity of hierarchical BiOX (X = Cl, Br, I) nanoplate microspheres. *J. Phys. Chem. C* **112**, 747–753. (doi:10.1021/jp077471t)
112. Gerstel P, Hoffmann RC, Lipowsky P, Jeurgens LPH, Bill J, Aldinger F. 2006 Mineralization from aqueous solutions of zinc salts directed by amino acids and peptides. *Chem. Mater.* **18**, 179–186. (doi:10.1021/cm051542o)
113. Goldman ER, Medintz IL, Hayhurst A, Anderson GP, Mauro JM, Iverson BL, Georgiou G, Mattoussi H. 2005 Quantum dot bioconjugates prepared using engineered poly-histidine terminated proteins. *Anal. Chim. Acta* **534**, 63–67. (doi:10.1016/j.aca.2004.03.079)
114. Yi GS, Sun B, Yang F, Chen D. 2001 Bionic synthesis of ZnS : Mn nanocrystals and their optical properties. *J. Mater. Chem.* **11**, 2928–2929. (doi:10.1039/b108394e)
115. Kho R *et al.* 2000 Zinc-histidine as nucleation centers for growth of ZnS nanocrystals. *Biochem. Biophys. Res. Commun.* **272**, 29–35. (doi:10.1006/bbrc.2000.2712)
116. Liu J, Hou X, Gao X, Ji X, Hu R, Shi Q. 1999 Thermal behaviour of the complexes of zinc amino acids. *J. Therm. Anal. Calorim.* **58**, 323–330. (doi:10.1023/A:1010142919232)
117. Qingzhi W, Chen X, Zhang P, Han Y, Chen X, Yan Y, Li S. 2008 Amino acid-assisted synthesis of ZnO hierarchical architectures and their novel photocatalytic activities. *Cryst. Growth Design* **8**, 3010–3018. (doi:10.1021/cg800126r)
118. Wu J, Duan F, Zheng Y, Xie Y. 2007 Synthesis of Bi_2WO_6 nanoplate-built hierarchical nest-like structures with visible-light-induced photocatalytic activity. *J. Phys. Chem. C* **111**, 12 866–12 871. (doi:10.1021/jp073877u)
119. Yu JG, Su YR, Cheng B. 2007 Template-free fabrication and enhanced photocatalytic activity of hierarchical macro-/mesoporous titania. *Adv. Funct. Mater.* **17**, 1984–1990. (doi:10.1002/adfm.200600933)
120. Baba T. 2007 Remember the light. *Nat. Photon.* **1**, 11–12. (doi:10.1038/nphoton.2006.58)
121. Norris DJ. 2007 Photonics crystals: a view of the future. *Nat. Mater.* **6**, 177–178. (doi:10.1038/nmat1844)
122. Miller DAB. 2006 Photonic crystals: straightening out light. *Nat. Mater.* **5**, 83–84. (doi:10.1038/nmat1566)
123. Tetreault N, Miguez H, Ozin GA. 2004 Dielectric planar defects in colloidal photonic crystal films. *Adv. Mater.* **16**, 346–349. (doi:10.1002/adma.200306361)
124. Hall N. 2003 Morphosynthesis of complex inorganic forms using pollen grain templates. *Chem. Commun.* 2784–2785. (doi:10.1039/b309877j)
125. Chen JIL *et al.* 2006 Amplified photochemistry with slow photons. *Adv. Mater.* **18**, 1915–1919. (doi:10.1002/adma.200600588)
126. Zhao TY, Liu Z, Nakata K, Nishimoto S, Murakami T, Zhao Y, Jiang L, Fujishima A. 2010 Multichannel TiO_2 hollow fibers with enhanced photocatalytic activity. *J. Mater. Chem.* **20**, 5095–5099. (doi:10.1039/c0jm00484g)
127. Li H, Bian Z, Zhu J, Zhang D, Li G, Huo Y, Li H, Lu Y. 2007 Mesoporous titania spheres with tunable chamber structure and enhanced photocatalytic activity. *J. Am. Chem. Soc.* **129**, 8406–8407. (doi:10.1021/ja072191c)